

Energy-Optimal Waypoint-Following Guidance Considering Autopilot Dynamics

SHAOMING HE 

HYO-SANG SHIN 

ANTONIOS TSOURDOS 

Cranfield University, Cranfield, U.K.

CHANG-HUN LEE 

Korea Advanced Institute of Science and Technology, Daejeon, South Korea

This article addresses the problem of energy-optimal waypoint-following guidance for an unmanned aerial vehicle, considering a general autopilot dynamics model. The proposed guidance law is derived as a solution of a linear-quadratic optimal control problem in conjunction with a linearized kinematics model. The algorithm developed integrates path planning and path following into a single step, and can be applied to a general waypoint-following mission. Theoretical analysis reveals that previously suggested optimal point-to-point guidance laws are special cases of the proposed approach. Nonlinear numerical simulations clearly demonstrate the effectiveness of the proposed formulations.

Manuscript received December 4, 2018; revised June 21, 2019; released for publication November 11, 2019. Date of publication November 28, 2019; date of current version August 7, 2020.

DOI. No. 10.1109/TAES.2019.2954149

Refereeing of this contribution was handled by D. Ghose.

Authors' addresses: S. He, H.-S. Shin, and A. Tsourdos are with the School of Aerospace, Transport and Manufacturing, Cranfield University, MK43 0AL, Cranfield, U.K., E-mail: (shaoming.he@cranfield.ac.uk; h.shin@cranfield.ac.uk; a.tsourdos@cranfield.ac.uk); C.-H. Lee is with the Department of Aerospace Engineering, Korea Advanced Institute of Science and Technology, Daejeon 34141, South Korea, E-mail: (lckdgn@kaist.ac.kr). (*Corresponding author: Hyo-Sang Shin.*)

0018-9251 © 2019 CCBY

I. INTRODUCTION

Unmanned aerial vehicles (UAVs) have been successfully deployed and show great potential in both civil and military applications. One of the fundamental enablers for UAVs to achieve high-level autonomy is to reach its destination with desired path constraints, e.g., waypoint and passing angle constraints [1]–[4]. Even though there exists a long history in this domain, complicated numerical trajectory optimization is usually utilized to find the energy- or time-optimal path of a UAV [5]–[12]. Numerical optimization, however, requires high-computational onboard power and, therefore, might not be suitable to ever-growing small-scale UAVs. For this reason, finding an analytical guidance algorithm is more beneficial for low-cost UAVs.

Over the past few years, the control-theoretic error-feedback-regulation concept was found to be widely accepted in the path-following guidance law design. The basic idea of this type of guidance law is to use the well-established control theories to force the trajectory tracking errors to converge to zero asymptotically or in finite time. In the view of this fact, the error-feedback-regulation method requires separate path-planning and path-following modules. In [13], the vector field approach was utilized to generate the heading command to guide the UAV to converge to a predesigned path asymptotically. Inspired by the concept of pursuit guidance, Park *et al.* [14], [15] suggested a nonlinear path-following guidance law, which guarantees asymptotical convergence of the lateral distance error. As an extension of [15], a three-dimensional nonlinear guidance law for UAV path following was developed in [16] based on the differential geometry. Considering the windy effect, a path-following guidance law, that combines the pursuit guidance concept and line-of-sight (LOS) guidance philosophy, was developed in [17]. By placing a synthetic waypoint on the desired trajectory, the authors of [18] and [19] proposed a synthetic waypoint guidance law (SWGL) for path following. The implementation of SWGL requires to tune the time-varying look-ahead distance, which determines the desired time horizon for the UAV to initiate a response to path changes. This time horizon specifies the prediction of set point and plays a similar role as the prediction horizons in model-predictive control (MPC). The SWGL algorithm, however, has some certain steady-state distance error when following a curved path. To alleviate this issue, Ratnoo *et al.* [20], [21] leveraged a trajectory shaping waypoint guidance law (TSWGL) to follow a virtual target. This algorithm is proved to generate the same instantaneous radius of curvature of a curved path and, therefore, is able to guarantee accurate path following.

Path following has also been investigated from the perspective of optimal control theory. As a desired path is usually defined in terms of a set of waypoints that a UAV has to visit sequentially, classical energy-optimal point-to-point guidance laws [22]–[26] can be easily adapted to path-following missions by applying them between every two consecutive points. However, it is unclear whether this simple strategy provides global optimality when

considering all waypoints. In [27]–[29], the authors formulated path following as a finite-horizon regulation problem and leveraged the systematic MPC to solve this optimal control problem. Similar to error-feedback-regulation strategies, the lateral distance tracking error was utilized as the system state in the MPC solution. By connecting every two consecutive waypoints through a straight line, a linear–quadratic optimal waypoint-following guidance was proposed in [30]. To generate a smoother trajectory at each waypoint, i.e., avoiding an abrupt change of the guidance command, the authors also derived the optimal line segment switching condition via minimizing the control magnitude. However, this algorithm fails to guarantee global optimality when considering the entire flight envelop. In [31], Ryoo *et al.* revealed that the energy-optimal waypoint-following problem is equivalent to applying the optimal terminal acceleration constrained impact angle guidance to every two consecutive waypoints in conjunction with proper boundary conditions. These boundary constraints, e.g., passing angle and passing acceleration, can be obtained through parameter optimization using numerical approaches.

Except for energy optimal guidance, time-optimal guidance has also been widely studied in the past few years. For point-to-point guidance, it is possible to exploit the geometry of extreme paths to find the analytic solution of time-optimal guidance [32]–[35]. However, when there are more than two waypoints, finding analytic solutions of the time-optimal guidance problem is generally difficult. For this reason, both heuristic [36] and suboptimal [37] algorithms were reported to find approximate solutions. Manyam *et al.* [38], [39] proposed an approximate time-optimal algorithm that guides the UAV to pass a given sequence of target waypoints in consideration of turning limit. This algorithm provides a tight lower bound to the generalized Dubins path problem. Unlike the original Dubins problem, Hota and Ghose [40], [41] investigated the problem of time-optimal trajectory generation from an initial point to a rectilinear path. The main difficulty in applying time-optimal guidance is that it is difficult to formulate the command into a state-feedback form. This means that numerical algorithms are required to calculate the guidance command at each time instant, which is generally not computationally efficient for vehicles with limited computational power.

Notice that most of the waypoint-following guidance laws were devised for a lag-free system. In practice, these guidance laws could inevitably experience performance degradation, such as a significant miss distance and a passing angle error associated with the waypoint, resulted from an autopilot lag in the guidance loop. Although Ryoo *et al.* [31] considered a first-order lag autopilot dynamics model in the guidance law design for waypoint following, the resultant guidance command is not explicitly provided and requires numerical parameter optimization in practical implementation. Motivated by these observations, this article aims to propose an analytical energy-optimal waypoint-following guidance law considering a general autopilot lag model. The formulation of the

proposed guidance law is based on a reduced-order linearized kinematics model through the terminal projection technique. The commanded acceleration is then analytically derived as a solution of a finite-time linear regulation problem using optimal control theory. The guidance command generated by the proposed algorithm is continuous, and there is no sudden change during waypoint change. This helps to reduce the transient effect when passing one waypoint. The proposed guidance law is generic, and theoretical analysis reveals that classical optimal point-to-point guidance laws [22]–[25] are special cases of the proposed algorithm. To the best of our knowledge, no closed-form solution that addresses the problem of global energy-optimal waypoint following in consideration of a general autopilot is available in the existing literature. Extensive empirical tests reveal that compensating autopilot lag will improve the performance of UAVs with large time lag and high speed.

The key features of the proposed guidance law are twofold. On one hand, the algorithm developed considers the command response lag and thus guarantees a finite guidance command. This prevents the divergence of the guidance command near the waypoint, and consequently, it offers advantages of reducing the miss distances and arrival angle errors associated with the waypoints. On the other hand, the proposed guidance law integrates path planning and path following into a single step, which differs from existing error-feedback-regulation approaches. This advantage is beneficial to reduce the design complexity for initial mission analysis.

The remainder of this article is organized as follows. The backgrounds and preliminaries of this article are stated in Section II. Section III presents the detailed derivation of the proposed guidance law. Section IV provides some particular cases of the proposed approach, followed by some property analysis shown in Section V. Some simulation results are presented in Section VI. Section VII concludes this article.

II. BACKGROUNDS AND PRELIMINARIES

This section first presents the nonlinear and linearized kinematics models that are utilized in guidance law derivation. Then, the problem formulation of this article is stated.

A. Nonlinear Kinematics

Consider there exist N waypoints that the UAV has to visit sequentially. This article considers a two-dimensional (2-D) geometry in an inertial coordinate XOY , shown in Fig. 1, since typical waypoint-following missions are usually carried out in the horizontal plane [31]. The symbols U and W_i denote the UAV and the i th waypoint, respectively. The variables r_i and σ_i represent the relative range and the LOS angle between the UAV and the i th waypoint, respectively. The notation θ stands for the UAV's flight path angle. The UAV changes its velocity V direction through the lateral acceleration a . Based on Fig. 1, the nonlinear

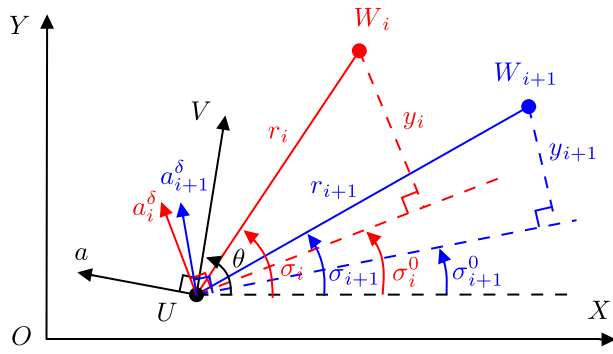


Fig. 1. Planar homing engagement geometry.

kinematics model can be formulated as

$$\begin{aligned} \dot{r}_i &= -V \cos(\theta - \sigma_i) \\ \dot{\sigma}_i &= -\frac{V \sin(\theta - \sigma_i)}{r_i} \\ \dot{\theta} &= \frac{a}{V}, \quad i \in [N] \end{aligned} \quad (1)$$

where $[N] \triangleq \{1, 2, \dots, N\}$.

In general, the UAV speed is predetermined according to the specific mission objective and is maintained by an engine controller. For this reason, we assume that the UAV is flying with a constant velocity for simplicity. In practice, the lateral acceleration a is generated by an autopilot, or flight control system, which has inevitable time delays. To account for the adverse effect of autopilot delay, it is worthy to consider the autopilot dynamics in the guidance law design. For this purpose, consider the UAV autopilot dynamics as the following arbitrary-order linear equations:

$$\begin{aligned} \dot{\mathbf{x}}_a &= \mathbf{A}_a \mathbf{x}_a + \mathbf{B}_a a_c \\ a &= \mathbf{C}_a \mathbf{x}_a + \mathbf{D}_a a_c \end{aligned} \quad (2)$$

where a_c represents the guidance command generated by the guidance law, $\mathbf{x}_a \in \mathbb{R}^{n_a \times 1}$ is the autopilot dynamics state vector, and \mathbf{A}_a , \mathbf{B}_a , \mathbf{C}_a , and \mathbf{D}_a are some proper autopilot dynamics matrices.

B. Passing Time

Without loss of generality, assume that the N waypoints are ordered by the increase of their corresponding passing times $t_{f,i}$ as $t_{f,i} < t_{f,i+1}$. Around the ideal approaching course, e.g., when the heading error becomes small, the waypoint passing time can be approximated by

$$t_{f,i} = t + t_{go,i} \quad (3)$$

where $t_{go,i} \triangleq r_i/V$ denotes the remaining flight time, or the so-called time-to-go, to pass the i th waypoint.

C. Linearized Kinematics

The derivation of optimal guidance laws will be performed based on a linearized model around the desired approaching course in this article. To this end, define σ_i^0 as the initial LOS angle between the UAV and the i th waypoint,

and denote a_i^σ as the UAV acceleration normal to the initial LOS direction, determined by the UAV position and the i th waypoint. Let y_i be the relative displacement between the UAV and the i th waypoint normal to the initial LOS direction, as shown in Fig. 1. Then, the relative kinematics model can be expressed as

$$\begin{aligned} \dot{y}_i &= v_i \\ \dot{v}_i &= -a_i^\sigma = -a \cos(\theta - \sigma_i^0). \end{aligned} \quad (4)$$

To allow for guidance law derivation, we assume that the velocity lead angle associated with the i th waypoint is small, i.e., $\cos(\theta - \sigma_i^0) \approx \cos(\theta^0 - \sigma_i^0)$, with θ^0 being the initial value of θ . Notice that this assumption is widely accepted in the optimal guidance law design [23], [42]–[45]. The relative kinematics between the UAV and the i th waypoint can then be linearized as

$$\begin{aligned} \dot{y}_i &= v_i \\ \dot{v}_i &= -c_i a \end{aligned} \quad (5)$$

where $c_i = \cos(\theta^0 - \sigma_i^0)$.

Define $\mathbf{x}_i = [y_i, v_i, \theta, \mathbf{x}_a^T]^T \in \mathbb{R}^{(n_a+3) \times 1}$ and $\mathbf{x} = [\mathbf{x}_1, \mathbf{x}_2, \dots, \mathbf{x}_N]^T \in \mathbb{R}^{(n_a+3)N \times 1}$ as the system state vector. Then, the linearized equations of motion can be written in a compact matrix form as

$$\dot{\mathbf{x}} = \mathbf{A} \mathbf{x} + \mathbf{B} a_c \quad (6)$$

where $\mathbf{A} \in \mathbb{R}^{(n_a+3)N \times (n_a+3)N}$ is a block diagonal matrix, and $\mathbf{B} \in \mathbb{R}^{(n_a+3)N \times 1}$ is the control input matrix. These two matrices are defined as

$$\mathbf{A} = \text{diag}(\mathbf{A}_1, \mathbf{A}_2, \dots, \mathbf{A}_N), \quad \mathbf{B} = [\mathbf{B}_1^T, \mathbf{B}_2^T, \dots, \mathbf{B}_N^T]^T \quad (7)$$

where

$$\mathbf{A}_i = \begin{bmatrix} 0 & 1 & 0 & 0_{1 \times n_a} \\ 0 & 0 & 0 & -c_i \mathbf{C}_a \\ 0 & 0 & 0 & \frac{\mathbf{C}_a}{V} \\ 0_{n_a \times 1} & 0_{n_a \times 1} & 0_{n_a \times 1} & \mathbf{A}_a \end{bmatrix}, \quad \mathbf{B}_i = \begin{bmatrix} 0 \\ -c_i \mathbf{D}_a \\ \frac{\mathbf{D}_a}{V} \\ \mathbf{B}_a \end{bmatrix}. \quad (8)$$

D. Problem Formulation

In practice, the energy consumption is of paramount importance for a UAV, since it determines the endurance of the vehicle. For this reason, this article considers the following performance index:

$$\begin{aligned} J &= \int_t^{t_{f,N}} a_c^2(\tau) d\tau \\ &= \begin{cases} \sum_{i=1}^N \int_t^{t_{f,i}} a_c^2(\tau) d\tau, & t \leq t_{f,1} \\ \sum_{i=2}^N \int_t^{t_{f,i}} a_c^2(\tau) d\tau, & t_{f,1} < t \leq t_{f,2} \\ \vdots \\ \int_t^{t_{f,N}} a_c^2(\tau) d\tau, & t_{f,N-1} < t \leq t_{f,N}. \end{cases} \end{aligned} \quad (9)$$

It has also been shown that quantity (9) relates to the speed loss due to induced drag for aerodynamically controlled vehicles, e.g., fixed-wing UAVs [46]. Therefore, minimizing the quadratic energy consumption is a worthy

goal for the guidance law design. In a waypoint-following mission, one path constraint is that the UAV has to visit all characteristic waypoints with zero miss distance, i.e.,

$$y_i(t_{f,i}) = 0, \quad i \in [N]. \quad (10)$$

Additionally, the UAV might need to pass some certain waypoints with desired flight path angles for some specific purposes, such as obstacle avoidance in terrain navigation and hostile radar detection avoidance in surveillance. Hence, we also consider an additional path constraint as

$$\theta(t_{f,l(j)}) = \theta_{l(j)}^d, \quad j \in [M], \quad l(j) \in [N], \quad M \leq N \quad (11)$$

where $l(j)$ stands for the index of waypoints that have specific flight path angle constraints and $\theta_{l(j)}^d$ denotes the desired flight angle when the UAV passes the $l(j)$ th waypoint.

In summary, the aim of this article is to find an analytical guidance command solution to the following optimization problem.

PROBLEM 1 Find a_c that minimizes the performance index (9), subject to the kinematics model (6) and path constraints (10), (11).

III. GUIDANCE LAW DERIVATION

In this section, we first present a reduced-order system using terminal projection via state transformation. Then, the detailed derivation of the proposed guidance law and its implementation issue are provided.

A. Order Reduction

Before solving the optimization problem formulated, the system order is reduced first using the terminal projection technique, or the so-called zero-effort transformation [47]–[50]. Notice that the zero-effort transformation aims to find the terminal system state values with zero control input from the current time onward. Based on this concept, the terminal projection \mathbf{Z}_i of the system (6) at current time t can be readily obtained using the homogeneous solution as

$$\mathbf{Z}_i = \begin{cases} \mathbf{C}_i \Phi_i(t_{f,i}, t) \mathbf{x}_i, & t \leq t_{f,i} \\ \mathbf{Z}_i(t_{f,i}), & t > t_{f,i} \end{cases} \quad (12)$$

where $\Phi_i(t_{f,i}, t)$ denotes the transition matrix associated with matrix \mathbf{A}_i , and \mathbf{C}_i is a constant matrix that extracts appropriate elements from the system state vector.

To satisfy terminal constraints (10) and (11), one needs to extract two variables for each waypoint: zero-effort miss (ZEM) $Z_{1,i}$ and zero-effort angle (ZEA) $Z_{2,i}$. The ZEM and the ZEA, respectively, refer to the final relative distance associated with the i th waypoint and the final flight path angle, if the UAV will not apply any control from the current time onward. For this reason, the matrix \mathbf{C}_i is given by

$$\mathbf{C}_i = \begin{bmatrix} 1 & 0 & 0 & 0_{1 \times n_a} \\ 0 & 0 & 1 & 0_{1 \times n_a} \end{bmatrix}. \quad (13)$$

Since

$$\dot{\Phi}_i(t_{f,i}, t) = -\Phi_i(t_{f,i}, t) \mathbf{A}_i \quad (14)$$

the time derivative of the terminal projection is

$$\dot{\mathbf{Z}}_i = \begin{cases} \mathbf{C}_i \Phi_i(t_{f,i}, t) \mathbf{B}_i a_c, & t \leq t_{f,i} \\ \mathbf{0}, & t > t_{f,i}. \end{cases} \quad (15)$$

Notice that the system order now reduces from $(n_a + 3)N$ to $2N$, and the terminal constraints (10) and (11) can be alternatively expressed as

$$\begin{aligned} Z_{1,i}(t_{f,i}) &= 0, \quad i \in [N] \\ Z_{2,l(j)}(t_{f,l(j)}) &= \theta_{l(j)}^d, \quad j \in [M], \quad l(j) \in [N], \quad M \leq N. \end{aligned} \quad (16)$$

With the zero-effort state transformation, Problem 1 now reduces to the following optimization problem.

PROBLEM 2 Find a_c that minimizes the performance index (9), subject to the kinematics model (15) and the path constraint (16).

B. General Guidance Law Solution

Define $\mathbf{C}_i \Phi_i(t_{f,i}, t) \mathbf{B}_i = [-b_i(t), g_i(t)]^T$ for notation convenience. The dynamics of the transformed zero-effort system can be obtained using (15) as

$$\dot{Z}_{1,i} = \begin{cases} -b_i(t) a_c, & t \leq t_{f,i} \\ 0, & t > t_{f,i} \end{cases} \quad (17)$$

$$\dot{Z}_{2,i} = \begin{cases} g_i(t) a_c, & t \leq t_{f,i} \\ 0, & t > t_{f,i}. \end{cases} \quad (18)$$

The solution of differential equations (17) and (18) are given by

$$Z_{1,i}(t_{f,i}) - Z_{1,i}(t) = \int_t^{t_{f,i}} -b_i(\tau) a_c(\tau) d\tau, \quad t \leq t_{f,i} \quad (19)$$

$$Z_{2,i}(t_{f,i}) - Z_{2,i}(t) = \int_t^{t_{f,i}} g_i(\tau) a_c(\tau) d\tau, \quad t \leq t_{f,i}. \quad (20)$$

Imposing terminal constraint (16) on (19) and (20) gives

$$Z_{1,i}(t) = \int_t^{t_{f,i}} b_i(\tau) a_c(\tau) d\tau, \quad t \leq t_{f,i} \quad (21)$$

$$\theta_{l(j)}^d - Z_{2,l(j)}(t) = \int_t^{t_{f,l(j)}} g_{l(j)}(\tau) a_c(\tau) d\tau, \quad t \leq t_{f,l(j)}. \quad (22)$$

According to Lemma 1, shown in Appendix A, if the guidance command a_c is optimal in terms of energy minimization, then there exist $N + M$ Lagrange multipliers $\lambda_i, \beta_j, i \in [N], j \in [M]$, such that the lateral acceleration command can be formulated as

$$a_c = a_\lambda + a_\beta \quad (23)$$

with

$$a_\lambda = \begin{cases} \sum_{i=1}^N \lambda_i b_i(t), & t \leq t_{f,1} \\ \sum_{i=2}^N \lambda_i b_i(t), & t_{f,1} < t \leq t_{f,2} \\ \vdots \\ \lambda_N b_N(t), & t_{f,N-1} < t \leq t_{f,N} \end{cases}$$

$$a_\beta = \begin{cases} \sum_{j=1}^M \beta_j g_{l(j)}(t), & t \leq t_{f,l(1)} \\ \sum_{j=2}^M \beta_j g_{l(j)}(t), & t_{f,l(1)} < t \leq t_{f,l(2)} \\ \vdots \\ \beta_M g_{l(M)}(t), & t_{f,l(M-1)} < t \leq t_{f,l(M)} \end{cases} \quad (24)$$

where a_λ refers to the ZEM regulation term and a_β represents the ZEA regulation command.

Without loss of generality, we only consider the case $t \leq t_{f,1}$ in the following derivations. The solutions for $t > t_{f,1}$ can be easily obtained through similar procedures. Substituting (23) into (21) and (22) under condition $t \leq t_{f,1}$ results in

$$\begin{aligned} Z_{1,i} &= \sum_{i'=1}^N \lambda_{i'} \int_t^{t_{f,i}} b_i(\tau) b_{i'}(\tau) d\tau \\ &\quad + \sum_{j'=1}^M \beta_{j'} \int_t^{t_{f,i}} b_i(\tau) g_{l(j')}(\tau) d\tau \\ &= \sum_{i'=1}^N \lambda_{i'} \int_t^{t_{f,\min\{i,i'\}}} b_i(\tau) b_{i'}(\tau) d\tau \\ &\quad + \sum_{j'=1}^M \beta_{j'} \int_t^{t_{f,\min\{i,l(j')\}}} b_i(\tau) g_{l(j')}(\tau) d\tau \end{aligned} \quad (25)$$

$$\begin{aligned} \theta_{l(j)}^d - Z_{2,l(j)} &= \sum_{i'=1}^N \lambda_{i'} \int_t^{t_{f,l(j)}} g_{l(j)}(\tau) b_{i'}(\tau) d\tau \\ &\quad + \sum_{j'=1}^M \beta_{j'} \int_t^{t_{f,l(j)}} g_{l(j)}(\tau) g_{l(j')}(\tau) d\tau \\ &= \sum_{i'=1}^N \lambda_{i'} \int_t^{t_{f,\min\{i,l(j)\}}} g_{l(j)}(\tau) b_{i'}(\tau) d\tau \\ &\quad + \sum_{j'=1}^M \beta_{j'} \int_t^{t_{f,\min\{l(j),l(j')\}}} g_{l(j)}(\tau) g_{l(j')}(\tau) d\tau. \end{aligned} \quad (26)$$

Define $\lambda = [\lambda_1, \lambda_2, \dots, \lambda_N]^T$ and $\beta = [\beta_1, \beta_2, \dots, \beta_M]^T$ as two Lagrange multiplier vectors, and $e_z = [Z_{1,1}, Z_{1,2}, \dots, Z_{1,N}]^T$ and $e_\theta = [\theta_{l(1)}^d - Z_{2,l(1)}, \theta_{l(2)}^d - Z_{2,l(2)}, \dots, \theta_{l(M)}^d - Z_{2,l(M)}]^T$ as two state error vectors. Then, (25) and (26) can be rewritten as a compact matrix form as

$$G \begin{bmatrix} \lambda \\ \beta \end{bmatrix} = \begin{bmatrix} e_z \\ e_\theta \end{bmatrix}, \quad G = \begin{bmatrix} G_1 & G_{12} \\ G_{21} & G_2 \end{bmatrix} \quad (27)$$

where $G_1 = G_1^T = [g_1(i, j)] \in \mathbb{R}^{N \times N}$, with elements $g_1(i, j)$, $i \in [N]$, $j \in [N]$, being

$$g_1(i, j) = \int_t^{t_{f,\min\{i,j\}}} b_i(\tau) b_j(\tau) d\tau \quad (28)$$

and $G_{12} = G_{12}^T = [g_{12}(i, j)] \in \mathbb{R}^{N \times M}$, with elements $g_{12}(i, j)$, $i \in [N]$, $j \in [M]$, being

$$g_{12}(i, j) = \int_t^{t_{f,\min\{i,l(j)\}}} b_i(\tau) g_{l(j)}(\tau) d\tau \quad (29)$$

and $G_2 = G_2^T = [g_2(i, j)] \in \mathbb{R}^{M \times M}$, with elements $g_2(i, j)$, $i \in [M]$, $j \in [M]$, being

$$g_2(i, j) = \int_t^{t_{f,\min\{l(i),l(j)\}}} g_{l(i)}(\tau) g_{l(j)}(\tau) d\tau. \quad (30)$$

From (27), the Lagrange multiplier vectors λ and β can be obtained as

$$\begin{bmatrix} \lambda \\ \beta \end{bmatrix} = G^{-1} \begin{bmatrix} e_z \\ e_\theta \end{bmatrix}. \quad (31)$$

The explicit guidance command for $t \leq t_{f,1}$ can then be readily obtained by substituting (31) into (23) as

$$\begin{aligned} a_c &= \lambda^T [b_1, b_2, \dots, b_N]^T + \beta^T [g_{l(1)}, g_{l(2)}, \dots, g_{l(M)}]^T \\ &= \left(G^{-1} \begin{bmatrix} e_z \\ e_\theta \end{bmatrix} \right)^T [b_1, b_2, \dots, b_N, g_{l(1)}, g_{l(2)}, \dots, g_{l(M)}]^T. \end{aligned} \quad (32)$$

REMARK 1 It follows from (32) that the proposed guidance law is generic. For this reason, it can be applied to a general UAV waypoint-following guidance mission with an arbitrary number of waypoints and an arbitrary number of arrival angle constraints.

REMARK 2 Compared to numerical time-optimal algorithms [38], [39], the main advantage of the proposed guidance law is that it provides a closed-form state-feedback solution and, therefore, is more beneficial for online applications. However, the drawback of the proposed guidance law is that it is derived based on the assumption that there is no bound on the commanded acceleration. This means that the UAV acceleration under the proposed guidance law might be saturated due to physical constraints in practical applications, unlike turning rate constrained time-optimal solutions [38], [39]. One possible solution to accommodate this issue is to shape the guidance command by modifying the cost function as [51]

$$J = \int_t^{t_{f,N}} W(\tau) a_c^2(\tau) d\tau \quad (33)$$

where $W(t)$ is a proper weighting function to distribute the guidance command. Our future study will handle generalization of the proposed approach in consideration of a general weighting function.

C. Guidance Law Implementation

From (32), it can be noted that the implementation of the proposed guidance law requires the information on the ZEM

and the ZEA. This information, however, cannot be directly measured from the UAV's onboard sensors. For this reason, this subsection will transform the guidance command into an equivalent form, which is a function of the measured signals $\dot{\sigma}_i$, V , r_i , θ , and \mathbf{x}_a . Under the assumption that the angle $\sigma_i - \sigma_i^0$ is small, Fig. 1 reveals that

$$\sigma_i - \sigma_i^0 = \frac{y_i}{r_i}. \quad (34)$$

Taking the time derivative of (34) results in

$$\dot{\sigma}_i = \frac{y_i + v_i t_{go,i}}{V t_{go,i}^2}. \quad (35)$$

Notice that the state transmission matrix $\Phi_i(t_{f,i}, t)$ can be written as

$$\Phi_i(t_{f,i}, t) = \begin{bmatrix} 1 & t_{f,i} - t & 0 & \Phi_{i,1}(t_{f,i}, t) \\ 0 & 1 & 0 & \Phi_{i,2}(t_{f,i}, t) \\ 0 & 0 & 1 & \Phi_{i,3}(t_{f,i}, t) \\ 0_{n_a \times 1} & 0_{n_a \times 1} & 0_{n_a \times 1} & \Phi_{i,4}(t_{f,i}, t) \end{bmatrix}. \quad (36)$$

Using (12) and (35), the zero-effort system states can then be formulated in an alternative form as

$$Z_{1,i} = \begin{cases} V \dot{\sigma}_i t_{go,i}^2 + \Phi_{i,1}(t_{f,i}, t) \mathbf{x}_a, & t \leq t_{f,i} \\ Z_{1,i}(t_{f,i}), & t > t_{f,i} \end{cases} \quad (37)$$

$$Z_{2,i} = \begin{cases} \theta + \Phi_{i,3}(t_{f,i}, t) \mathbf{x}_a, & t \leq t_{f,i} \\ Z_{2,i}(t_{f,i}), & t > t_{f,i}. \end{cases} \quad (38)$$

Substituting (37) and (38) into (32) gives the guidance command in terms of measured signals $\dot{\sigma}_i$, V , r_i , θ , and \mathbf{x}_a . This supports the practical application of the proposed guidance law. Note that although the proposed guidance law is derived based on the linearized engagement kinematics, the error generated in the linearization process can be alleviated by using (37) and (38) in implementation, since (37) and (38) transform the original linear terms into their corresponding nonlinear expressions [52].

IV. SOME PARTICULAR CASES

This section discusses some particular cases of the proposed guidance law. For simplicity, we consider ideal autopilot dynamics and first-order autopilot dynamics cases here.

A. Ideal Autopilot Dynamics

If the UAV's autopilot dynamics is ideal, that is,

$$\mathbf{A}_a = 0, \quad \mathbf{B}_a = 0, \quad \mathbf{C}_a = 0, \quad \mathbf{D}_a = 1 \quad (39)$$

then we have

$$Z_{1,i} = \begin{cases} V \dot{\sigma}_i t_{go,i}^2, & t \leq t_{f,i} \\ Z_{1,i}(t_{f,i}), & t > t_{f,i} \end{cases} \quad (40)$$

$$Z_{2,i} = \begin{cases} \theta, & t \leq t_{f,i} \\ Z_{2,i}(t_{f,i}), & t > t_{f,i} \end{cases} \quad (41)$$

$$b_i(t) = c_i t_{go,i}, \quad g_i(t) = \frac{1}{V}. \quad (42)$$

The integrals in (25) and (26) for this simple case can be easily obtained as

$$\begin{aligned} & \int_t^{t_{f,\min\{i,i'\}}} b_i(\tau) b_{i'}(\tau) d\tau \\ &= \frac{c_i c_{i'} t_{go,\min\{i,i'\}}^2}{6} (2t_{go,\min\{i,i'\}} + 3d_{i,i'}) \end{aligned} \quad (43)$$

$$\begin{aligned} & \int_t^{t_{f,\min\{i,l(j')\}}} b_i(\tau) g_{l(j')}(\tau) d\tau \\ &= \begin{cases} \frac{c_i t_{go,i}^2}{2V}, & i \leq l(j') \\ \frac{c_i t_{go,l(j')}^2}{2V} + \frac{c_i d_{i,l(j')} t_{go,l(j')}}{V}, & i > l(j') \end{cases} \end{aligned} \quad (44)$$

$$\int_t^{t_{f,\min\{l(j),l(j')\}}} g_{l(j)}(\tau) g_{l(j')}(\tau) d\tau = \frac{t_{go,\min\{l(j),l(j')\}}}{V^2} \quad (45)$$

where $d_{i,i'} = t_{f,\max\{i,i'\}} - t_{f,\min\{i,i'\}}$.

Substituting (40)–(45) into (32) gives the guidance command for $t \leq t_{f,1}$ as

$$\begin{aligned} a_c &= \boldsymbol{\lambda}^T [c_1 t_{go,1}, c_2 t_{go,2}, \dots, c_N t_{go,N}]^T \\ &+ \boldsymbol{\beta}^T \underbrace{\left[\frac{1}{V}, \frac{1}{V}, \dots, \frac{1}{V} \right]^T}_{M \text{ elements}} \\ &= \left(\mathbf{G}^{-1} \begin{bmatrix} e_z \\ e_\theta \end{bmatrix} \right)^T \\ &\times \left[c_1 t_{go,1}, c_2 t_{go,2}, \dots, c_N t_{go,N}, \underbrace{\frac{1}{V}, \frac{1}{V}, \dots, \frac{1}{V}}_{M \text{ elements}} \right]^T \end{aligned} \quad (46)$$

which is called lag-free energy-optimal waypoint-following guidance law (OWFGL-0).

B. First-Order Autopilot Dynamics

Assume that the UAV autopilot is modeled by a first-order dynamics, that is,

$$\mathbf{A}_a = -\frac{1}{\tau_a}, \quad \mathbf{B}_a = \frac{1}{\tau_a}, \quad \mathbf{C}_a = 1, \quad \mathbf{D}_a = 0 \quad (47)$$

where τ_a denotes the autopilot time constant.

Then, the transition matrix is determined as

$$\Phi_i(t_{f,i}, t) = \begin{bmatrix} 1 & t_{f,i} - t & 0 & -\tau_a^2 \phi\left(\frac{t_{f,i}-t}{\tau_a}\right) \\ 0 & 1 & 0 & \tau_a \left(e^{-\frac{t_{f,i}-t}{\tau_a}} - 1\right) \\ 0 & 0 & 1 & \frac{\tau_a}{V} \left(1 - e^{-\frac{t_{f,i}-t}{\tau_a}}\right) \\ 0 & 0 & 0 & e^{-\frac{t_{f,i}-t}{\tau_a}} \end{bmatrix} \quad (48)$$

which generates the following zero-effort transformations:

$$Z_{1,i} = \begin{cases} V \dot{\sigma}_i t_{go,i}^2 - c_i \tau_a^2 \phi\left(\frac{t_{go,i}}{\tau_a}\right) a, & t \leq t_{f,i} \\ Z_{1,i}(t_{f,i}), & t > t_{f,i} \end{cases} \quad (49)$$

$$Z_{2,i} = \begin{cases} \theta + \frac{\tau_a}{V} \left(1 - e^{-\frac{t_{go,i}}{\tau_a}}\right) a, & t \leq t_{f,i} \\ Z_{2,i}(t_{f,i}), & t > t_{f,i} \end{cases} \quad (50)$$

$$b_i(t) = c_i \tau_a \phi\left(\frac{t_{go,i}}{\tau_a}\right), \quad g_i(t) = \frac{1 - e^{-\frac{t_{go,i}}{\tau_a}}}{V} \quad (51)$$

where $\phi(x) \triangleq e^{-x} + x - 1$.

After some tedious but simple algebra manipulations, the integrals in (25) and (26) are determined as (52)–(54) shown at the bottom of this page.

The explicit guidance command can then be readily obtained by substituting (49)–(54) into (32). This guidance command is termed as the first-order lag energy-optimal waypoint-following guidance law (OWFGL-1) in this article.

REMARK 3 For higher order autopilot systems, i.e., $n_a > 1$, the integrals in (25) and (26) are algebraically complicated. However, the resultant expressions can be easily evaluated using an algebraic mathematical solver such as Mathematica.

V. RELATIONSHIP WITH POINT-TO-POINT OPTIMAL GUIDANCE LAWS

This section analyzes the relationship between the proposed guidance law and classical point-to-point optimal guidance laws [22]–[25]. For the purpose of illustration, a first-order lag autopilot system is considered here.

A. $N = 1$ and $M = 0$

When there exists only one waypoint to be visited by the UAV without any specified flight path, the original optimization problem reduces to the energy-optimal point-to-point interception problem. Then, the guidance command of the proposed guidance law, shown in (23), reduces to

$$a_c = \lambda_1 b_1 = \lambda_1 \tau_a \phi\left(\frac{t_{go,1}}{\tau_a}\right). \quad (55)$$

Note that matrix \mathbf{G} under conditions $N = 1$ and $M = 0$ reduces to a scalar G as

$$G = \frac{\tau_a^3}{2} \left(1 - e^{-\frac{2t_{go,1}}{\tau_a}}\right) - 2\tau_a^2 t_{go,1} e^{-\frac{t_{go,1}}{\tau_a}} + \frac{t_{go,1}^3}{3} - \tau_a t_{go,1}^2 + \tau_a^2 t_{go,1}. \quad (56)$$

From (31), we can readily solve the Lagrange multiplier as

$$\lambda_1 = \frac{Z_{1,1}}{\frac{\tau_a^3}{2} \left(1 - e^{-\frac{2t_{go,1}}{\tau_a}}\right) - 2\tau_a^2 t_{go,1} e^{-\frac{t_{go,1}}{\tau_a}} + \frac{t_{go,1}^3}{3} - \tau_a t_{go,1}^2 + \tau_a^2 t_{go,1}}. \quad (57)$$

Substituting (57) into (55) gives the explicit guidance command as

$$a_c = \frac{N_1 Z_{1,1}}{t_{go,1}^2} \quad (58)$$

with

$$N_1 = \frac{\phi\left(\frac{t_{go,1}}{\tau_a}\right)}{\frac{\tau_a^2}{2t_{go,1}^2} \left(1 - e^{-\frac{2t_{go,1}}{\tau_a}}\right) - \frac{2\tau_a}{t_{go,1}} e^{-\frac{t_{go,1}}{\tau_a}} + \frac{3t_{go,1}}{\tau_a} - 1 + \frac{\tau_a}{t_{go,1}}} \quad (59)$$

$$\int_t^{t_{f,\min\{i,i'\}}} b_i(\tau) b_{i'}(\tau) d\tau = c_i c_{i'} \left[\frac{\tau_a^3}{2} \left(e^{-\frac{d_{i,i'}}{\tau_a}} - e^{-\frac{2t_{go,\min\{i,i'\}} + d_{i,i'}}{\tau_a}} \right) + \tau_a^2 d_{i,i'} \left(1 - e^{-\frac{t_{go,\min\{i,i'\}}}{\tau_a}} \right) - \tau_a^2 t_{go,\min\{i,i'\}} \left(e^{-\frac{t_{go,\min\{i,i'\}}}{\tau_a}} + e^{-\frac{t_{go,\min\{i,i'\}} + d_{i,i'}}{\tau_a}} \right) + \frac{t_{go,\min\{i,i'\}}^2}{6} (2t_{go,\min\{i,i'\}} + 3d_{i,i'}) - \tau_a t_{go,\min\{i,i'\}}^2 - \tau_a d_{i,i'} t_{go,\min\{i,i'\}} + \tau_a^2 t_{go,\min\{i,i'\}} \right] \quad (52)$$

$$\int_t^{t_{f,\min\{i,l(j')\}}} b_i(\tau) g_{l(j')}(\tau) d\tau = \begin{cases} \frac{c_i \tau_a}{V} \left[\tau_a - t_{go,i} + \frac{t_{go,i}^2}{2\tau_a} - \frac{\tau_a}{2} e^{-\frac{d_{i,l(j')}}{\tau_a}} - \tau_a e^{-\frac{t_{go,i}}{\tau_a}} + t_{go,i} e^{-\frac{t_{go,i} + d_{i,l(j')}}{\tau_a}} + \frac{\tau_a}{2} e^{-\frac{2t_{go,i} + d_{i,l(j')}}{\tau_a}} \right], & i \leq l(j') \\ \frac{c_i}{2V} \left[\tau_a^2 e^{-\frac{d_{i,l(j')}}{\tau_a}} - \tau_a^2 e^{-\frac{2t_{go,l(j')} + d_{i,l(j')}}{\tau_a}} - 2d_{i,l(j')} \tau_a + 2d_{i,l(j')} t_{go,l(j')} - 2\tau_a t_{go,l(j')} + t_{go,l(j')}^2 - 2\tau_a^2 e^{-\frac{t_{go,l(j')}}{\tau_a}} + 2\tau_a d_{i,l(j')} e^{-\frac{t_{go,l(j')}}{\tau_a}} + 2\tau_a t_{go,l(j')} e^{-\frac{t_{go,l(j')}}{\tau_a}} \right], & i > l(j') \end{cases} \quad (53)$$

$$\int_t^{t_{f,\min\{l(j),l(j')\}}} g_{l(j)}(\tau) g_{l(j')}(\tau) d\tau = \frac{1}{V^2} \left[\tau_a \phi\left(\frac{t_{go,\min\{l(j),l(j')\}}}{\tau_a}\right) + \tau_a e^{-\frac{t_{go,\min\{l(j),l(j')\}} + d_{l(j),l(j')}}{\tau_a}} - \frac{\tau_a}{2} e^{-\frac{d_{l(j),l(j')}}{\tau_a}} - \frac{\tau_a}{2} e^{-\frac{2t_{go,\min\{l(j),l(j')\}} + d_{l(j),l(j')}}{\tau_a}} \right] \quad (54)$$

which coincides with the energy-optimal point-to-point intercept guidance with first-order autopilot dynamics proposed in [22] and [23].

B. $N = 2$ and $M = 0$

To provide better understanding of the structure and nature of the proposed guidance law, we consider a special case with $N = 2$ and $M = 0$, e.g., the UAV is required to visit two waypoints sequentially without any arrival angle constraints. Under this condition, the guidance command of the proposed guidance law (23) for $t \leq t_{f,1}$ reduces to

$$a_c = \lambda_1 b_1 + \lambda_2 b_2 = \lambda_1 \tau_a \phi\left(\frac{t_{go,1}}{\tau_a}\right) + \lambda_2 \tau_a \phi\left(\frac{t_{go,2}}{\tau_a}\right). \quad (60)$$

The matrix \mathbf{G} with $N = 2$ and $M = 0$ is given by

$$\mathbf{G} = \begin{bmatrix} g_1 & g_{12} \\ g_{21} & g_2 \end{bmatrix} \quad (61)$$

where

$$\begin{aligned} g_1 &= \frac{\tau_a^3}{2} \left(1 - e^{-\frac{2t_{go,1}}{\tau_a}}\right) - 2\tau_a^2 t_{go,1} e^{-\frac{t_{go,1}}{\tau_a}} \\ &\quad + \frac{t_{go,1}^3}{3} - \tau_a t_{go,1}^2 + \tau_a^2 t_{go,1} \\ g_{12} &= g_{21} = \frac{\tau_a^3}{2} \left(e^{-\frac{d_{1,2}}{\tau_a}} - e^{-\frac{2t_{go,1}+d_{1,2}}{\tau_a}}\right) \\ &\quad - \tau_a^2 t_{go,1} \left(e^{-\frac{t_{go,1}}{\tau_a}} + e^{-\frac{t_{go,1}+d_{1,2}}{\tau_a}}\right) \\ &\quad + \tau_a^2 d_{1,2} \left(1 - e^{-\frac{t_{go,1}}{\tau_a}}\right) + \frac{t_{go,1}^2}{6} (2t_{go,1} + 3d_{1,2}) \\ &\quad - \tau_a t_{go,1}^2 - \tau_a t_{go,1} d_{1,2} + \tau_a^2 t_{go,1} \\ g_2 &= \frac{\tau_a^3}{2} \left(1 - e^{-\frac{2t_{go,2}}{\tau_a}}\right) - 2\tau_a^2 t_{go,2} e^{-\frac{t_{go,2}}{\tau_a}} + \frac{t_{go,2}^3}{3} \\ &\quad - \tau_a t_{go,2}^2 + \tau_a^2 t_{go,2} \end{aligned} \quad (62)$$

with $d_{1,2} = t_{go,2} - t_{go,1}$.

Using (31), the Lagrange multipliers can be formulated as

$$\begin{aligned} \begin{bmatrix} \lambda_1 \\ \lambda_2 \end{bmatrix} &= \begin{bmatrix} g_1 & g_{12} \\ g_{21} & g_2 \end{bmatrix}^{-1} \begin{bmatrix} Z_{1,1} \\ Z_{1,2} \end{bmatrix} \\ &= \frac{1}{\Lambda} \begin{bmatrix} g_2 Z_{1,1} - g_{12} Z_{1,2} \\ -g_{21} Z_{1,1} + g_1 Z_{1,2} \end{bmatrix} \end{aligned} \quad (63)$$

where $\Lambda = g_1 g_2 - g_{12}^2$.

The guidance command for $t \leq t_{f,1}$ can be readily obtained by substituting (63) into (60) as

$$a_c = \frac{N_1 Z_{1,1}}{t_{go,1}^2} + \frac{N_2 Z_{1,2}}{t_{go,2}^2} \quad (64)$$

where

$$N_1 = \frac{\tau_a t_{go,1}^2}{\Lambda} \left[g_2 \phi\left(\frac{t_{go,1}}{\tau_a}\right) - g_{21} \phi\left(\frac{t_{go,2}}{\tau_a}\right) \right]$$

$$N_2 = \frac{\tau_a t_{go,2}^2}{\Lambda} \left[g_1 \phi\left(\frac{t_{go,2}}{\tau_a}\right) - g_{12} \phi\left(\frac{t_{go,1}}{\tau_a}\right) \right]. \quad (65)$$

Introducing the biased term $a_B = N_2 Z_{1,2} / t_{go,2}^2$, guidance command (64) can then be formulated in an alternative form as

$$a_c = \frac{N_1 Z_{1,1}}{t_{go,1}^2} + a_B \quad (66)$$

which can be viewed as a general ZEM shaping guidance law $N_1 Z_{1,1} / t_{go,1}^2$ [52] with a biased term a_B . From (65), it can be easily verified that the biased term a_B gradually becomes the dominant part when the UAV approaches the first waypoint.

Recalling the results derived for $N = 1$ and $M = 0$, the guidance command when $t_{f,1} < t \leq t_{f,2}$ for the case of $N = 2$ and $M = 0$ is given by

$$a_c = \frac{N'_2 Z_{1,2}}{t_{go,2}^2} \quad (67)$$

with

$$N'_2 = \frac{\phi\left(\frac{t_{go,2}}{\tau_a}\right)}{\frac{\tau_a^2}{2t_{go,2}^2} \left(1 - e^{-\frac{2t_{go,2}}{\tau_a}}\right) - \frac{2\tau_a}{t_{go,2}} e^{-\frac{t_{go,2}}{\tau_a}} + \frac{3t_{go,2}}{\tau_a} - 1 + \frac{\tau_a}{t_{go,2}}}. \quad (68)$$

In summary, the guidance command for $N = 2$ and $M = 0$ is determined as

$$a_c = \begin{cases} \frac{N_1 Z_{1,1}}{t_{go,1}^2} + \frac{N_2 Z_{1,2}}{t_{go,2}^2}, & t \leq t_{f,1} \\ \frac{N'_2 Z_{1,2}}{t_{go,2}^2}, & t_{f,1} < t \leq t_{f,2}. \end{cases} \quad (69)$$

C. $N = 1$ and $M = 1$

When there exists only one waypoint to be visited by the UAV with a specified flight path θ_1^d , the original optimization problem reduces to the energy-optimal point-to-point rendezvous problem. Then, the guidance command of the proposed guidance law, shown in (23), can be formulated as

$$a_c = \lambda_1 b_1 + \beta_1 g_1 = \lambda_1 \tau_a \phi\left(\frac{t_{go,1}}{\tau_a}\right) + \beta_1 \frac{1 - e^{-\frac{t_{go,1}}{\tau_a}}}{V}. \quad (70)$$

Under conditions $N = 1$ and $M = 1$, the matrix \mathbf{G} becomes

$$\mathbf{G} = \begin{bmatrix} g_1 & g_{12} \\ g_{21} & g_2 \end{bmatrix} \quad (71)$$

where

$$\begin{aligned} g_1 &= \frac{\tau_a^3}{2} \left(1 - e^{-\frac{2t_{go,1}}{\tau_a}}\right) - 2\tau_a^2 t_{go,1} e^{-\frac{t_{go,1}}{\tau_a}} + \frac{t_{go,1}^3}{3} \\ &\quad - \tau_a t_{go,1}^2 + \tau_a^2 t_{go,1} \\ g_{12} &= g_{21} = \frac{\tau_a}{V} \left[\frac{\tau_a}{2} - t_{go,1} + \frac{t_{go,1}^2}{2\tau_a} - \tau_a e^{-\frac{t_{go,1}}{\tau_a}} \right. \\ &\quad \left. + t_{go,1} e^{-\frac{t_{go,1}}{\tau_a}} + \frac{\tau_a}{2} e^{-\frac{2t_{go,1}}{\tau_a}} \right] \end{aligned}$$

TABLE I
Inertial Positions of All Waypoints

Waypoint ID	Inertial position
1	(1000m, 500m)
2	(2000m, 750m)
3	(3000m, 1000m)
4	(4000m, 1500m)
5	(5000m, 1250m)
6	(6000m, 1750m)
7	(7000m, 2000m)
8	(8000m, 1500m)

$$g_2 = \frac{1}{V^2} \left[t_{go,1} + 2\tau_a e^{-\frac{t_{go,1}}{\tau_a}} - \frac{3\tau_a}{2} - \frac{\tau_a}{2} e^{-\frac{2t_{go,1}}{\tau_a}} \right]. \quad (72)$$

Using (31), the Lagrange multipliers can be formulated as

$$\begin{aligned} \begin{bmatrix} \lambda_1 \\ \beta_1 \end{bmatrix} &= \begin{bmatrix} g_1 & g_{12} \\ g_{21} & g_2 \end{bmatrix}^{-1} \begin{bmatrix} Z_{1,1} \\ \theta_1^d - Z_{2,1} \end{bmatrix} \\ &= \frac{1}{\Delta} \begin{bmatrix} g_2 Z_{1,1} - g_{12} (\theta_1^d - Z_{2,1}) \\ -g_{21} Z_{1,1} + g_1 (\theta_1^d - Z_{2,1}) \end{bmatrix} \end{aligned} \quad (73)$$

where $\Delta = g_1 g_2 - g_{12}^2$.

Substituting (73) into (70) gives the explicit guidance command as

$$a_c = \frac{K_1 Z_{1,1}}{t_{go,1}^2} + \frac{K_2 (\theta_1^d - Z_{2,1})}{t_{go,1}} \quad (74)$$

where

$$\begin{aligned} K_1 &= \frac{t_{go,1}^2}{\Delta} \left[\tau_a \phi \left(\frac{t_{go,1}}{\tau_a} \right) g_2 - \frac{1 - e^{-\frac{t_{go,1}}{\tau_a}}}{V} g_{21} \right] \\ K_2 &= \frac{t_{go,1}}{\Delta} \left[\frac{1 - e^{-\frac{t_{go,1}}{\tau_a}}}{V} g_1 - \tau_a \phi \left(\frac{t_{go,1}}{\tau_a} \right) g_{12} \right] \end{aligned} \quad (75)$$

which coincides with the energy-optimal point-to-point impact angle guidance law with first-order autopilot dynamics proposed in [24] and [25].

VI. NUMERICAL SIMULATIONS

In this section, nonlinear numerical simulations are performed to validate the proposed guidance law. In the considered scenario, a UAV with constant speed $V = 30$ m/s is required to pass eight waypoints, summarized in Table I. The UAV starts the mission at position (0 m, 0 m) with an initial flight path angle 30° . The UAV autopilot is modeled as a first-order lag system with time constant $\tau_a = 0.5$ s, which is enough to identify the characteristics of a guidance law in the conservative point of view.

A. Comparison With Other Waypoint Guidance Laws

To evaluate the energy-minimization property of the guidance law developed, this subsection compares the proposed OWFGL-1 algorithm with the SWGL [18], [19], the TSWGL [20], [21], and classical point-to-point optimal guidance laws with first-order autopilot dynamics (P2POGL-1) [22]–[25]. The guidance commands of both

SWGL and TSWGL are summarized in Appendix B. In the simulations, P2POGL-1 is applied to every two consecutive waypoints for path following. The guidance command of P2POGL-1 is defined as

$$a_c = \begin{cases} (74), & \text{if next waypoint requires a specific} \\ & \text{arrival angle} \\ (58), & \text{otherwise.} \end{cases}$$

We first consider the scenario without any passing angle constraint. The UAV flight trajectories obtained from different guidance laws are shown in Fig. 2(a). This figure reveals that the UAV guided by all guidance laws can successfully accomplish its waypoint-following mission at some extent. The quantitative comparison results of mean miss distance over all waypoints under different guidance laws for this scenario, are summarized in Table II. From this table, one can note that both P2POGL-1 and the proposed guidance law outperform the SWGL and the TSWGL in terms of guidance accuracy. The reason is that both P2POGL-1 and the proposed algorithm consider autopilot dynamics in guidance law derivation. Compared to other guidance laws, the flight path angle under the proposed guidance law is smoother and, therefore, is more beneficial for practical application, as confirmed by Fig. 2(b). Fig. 2(c) compares the acceleration response generated by these four different guidance laws through the onboard autopilot. From this figure, it is clear that the acceleration response under SWGL, TSWGL, and P2POGL-1 has sharp changes during waypoint switch. As a comparison, the achieved acceleration under the proposed guidance law is continuous and smooth during the entire flight period, which is more desirable for the onboard flight control system. The reason of this phenomenon is clear: b_i gradually converges to zero when the UAV approaches the i th waypoint. This means that the term $\lambda_i b_i$ in the guidance command gradually diminishes when $t_{go,i} \rightarrow 0$, which helps to reduce the transient effect when passing the i th waypoint. The energy consumption, defined as $J = \int_t^{t_{f,N}} a^2(\tau) d\tau$, obtained from different guidance laws is presented in Fig. 2(d). As shown in this figure, the proposed guidance law requires less energy consumption, compared with other guidance laws.

Now, let us analyze the characteristics of the proposed guidance law for scenarios with the flight path constraint. In the simulations, we assume that the UAV is required to pass the fourth waypoint with the desired flight path angle 0° and the eighth waypoint with the desired flight path angle -90° . Since SWGL and TSWGL cannot control the flight path angle of the UAV, we only compare the proposed guidance law with P2POGL-1 in this scenario. The UAV flight trajectories and flight path angle profiles obtained from P2POGL-1 as well as the proposed guidance law are shown in Fig. 3(a) and (b), respectively. These two figures reveal that the UAV guided by both guidance laws can successfully accomplish its waypoint-following mission. The quantitative comparison results of mean miss distance and mean passing angle over all waypoints under different guidance laws for this scenario, are summarized in Table III.

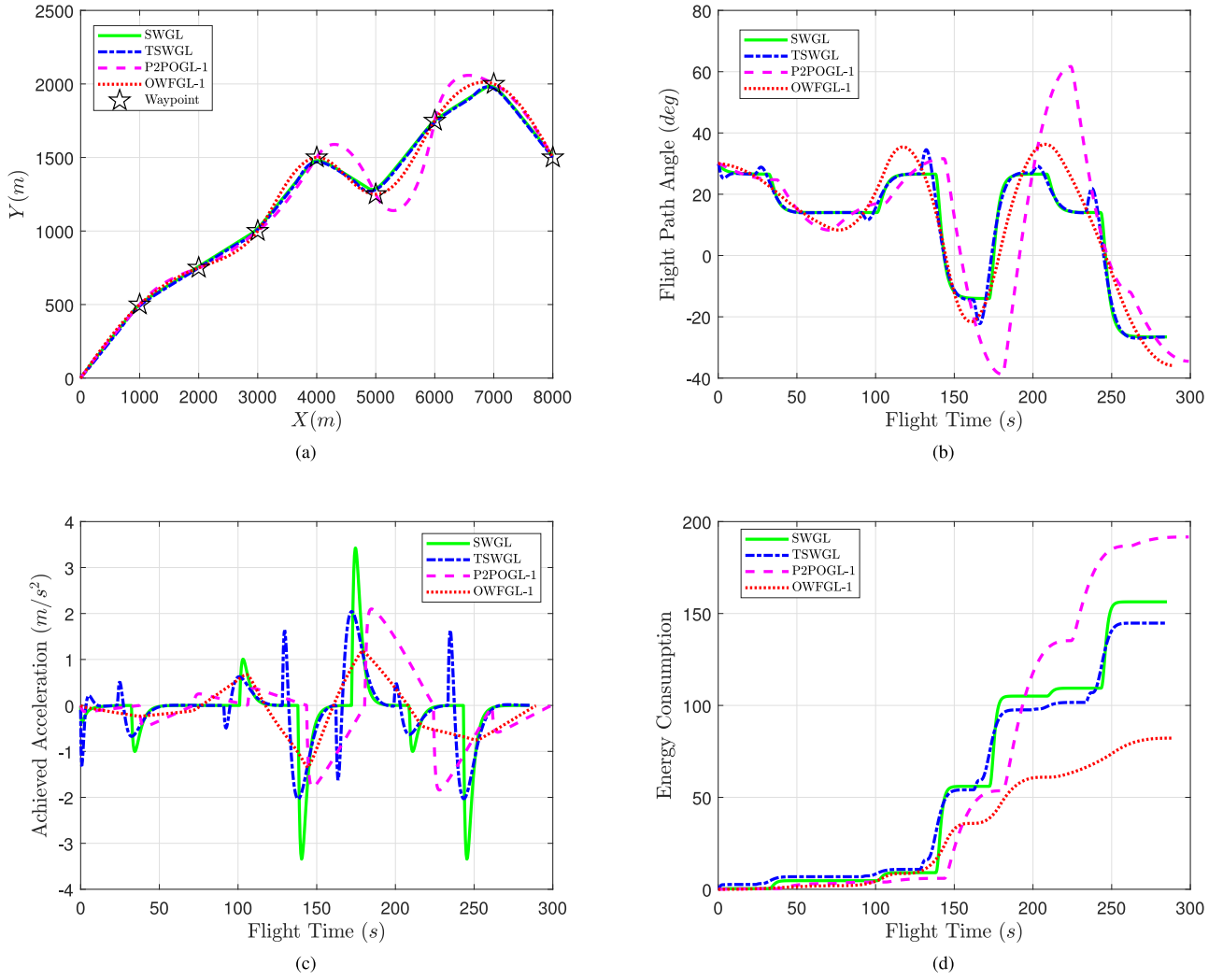


Fig. 2. Comparison of different guidance laws for waypoint following without flight path angle constraints. (a) Flight trajectory. (b) Flight path angle. (c) Acceleration response. (d) Energy consumption.

TABLE II
Comparison Results of Mean Miss Distance

Metric	SWGL	TSWGL	P2POGL-1	Proposed
Mean miss distance	9.2875m	4.2895m	0.1806m	0.1363m

The recorded miss distance and the flight path angle error obtained from both guidance laws are less than 0.2 m and 0.1° in our simulations. The achieved accelerations under both guidance laws are depicted in Fig. 3(c). This figure demonstrates that the acceleration response under P2POGL-1 exhibits suddenly large changes when the UAV passes one waypoint due to the discontinuity of P2POGL-1 at the switching point. As a comparison, the achieved acceleration under the proposed guidance law is smoother during the entire flight period, which is more desirable for the onboard flight control system. The reason can be attributed to the fact that both b_i and g_i converge to zero when the UAV approaches the i th waypoint, as deduced from (51).

This means that the commanded acceleration of the proposed guidance law is continuous, and therefore, there is no sudden command change during waypoint switch. Since both P2POGL-1 and the proposed OWFGL-1 consider autopilot dynamics in guidance law derivation, the bounded guidance command can be ensured during the flight. The energy consumption, defined as $J = \int_t^{t_f, N} a^2(\tau) d\tau$, obtained from different guidance laws is compared in Fig. 3(d). As shown in this figure, the proposed guidance law requires less energy consumption, compared to P2POGL-1. In the considered scenario, the proposed guidance law helps to reduce more than 25% energy consumption. Therefore, the UAV guided by the proposed approach is expected to have longer endurance than guided by P2POGL-1.

B. Effect of Autopilot Dynamics Compensation

To show the advantages of considering autopilot lag in the guidance law design, this subsection compares the performance of OWFGL-1 with that of OWFGL-0 under different conditions.

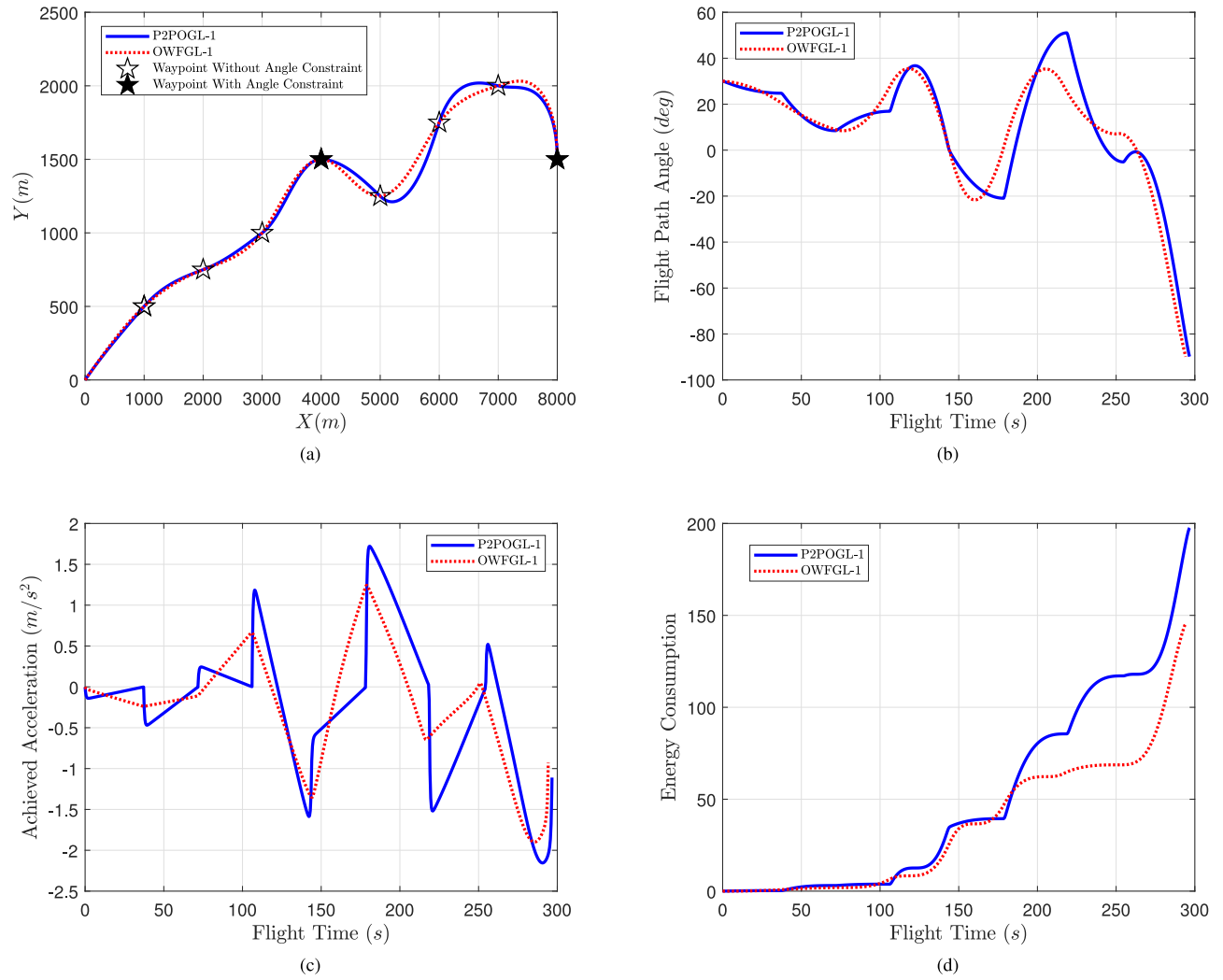


Fig. 3. Comparison of different guidance laws for waypoint following with partial flight path angle constraints. (a) Flight trajectory. (b) Flight path angle. (c) Acceleration response. (d) Energy consumption.

TABLE III
Comparison Results of the Mean Miss Distance and the Passing Angle Error

Metric	P2POGL-1	Proposed
Mean miss distance	0.1901m	0.1771m
Mean passing angle error	0.0398°	0.0239°

We first investigate the performance of the proposed guidance law under various time lags $\tau_a = 0.5, 1$, and 2 s with a fixed velocity $V = 30$ m/s. The simulation results, including UAV flight trajectories, flight angle profiles, achieved acceleration, and energy consumption, are shown in Fig. 4. As shown in Fig. 4(a) and (b), both guidance laws successfully drive the UAV to arrive the desired waypoints at some extent. Although the recorded passing angle error in OWFGL-1 is smaller than that in OWFGL-0 in our simulations, it is fair to state that both guidance laws

satisfy the arrival angle constraint in the considered scenario, as confirmed by Fig. 4(b). Fig. 4(c) indicates that the achieved acceleration of OWFGL-1 is smoother than that of OWFGL-0. Also notice from Fig. 4(c) that the guidance command of OWFGL-0 shows divergence when passing one waypoint, as the autopilot lag is neglected in the guidance law derivation, especially for the fourth and the fifth waypoints in the considered scenario. Such divergence may result in a large miss distance and a significant passing angle error near the waypoint. On the other hand, the OWFGL-1 algorithm can successfully compensate the autopilot lag, and the acceleration command does not diverge, as shown in Fig. 4(c). Due to the introduced guidance command divergence, the energy consumption of OWFGL-0 is higher than that of OWFGL-1, as shown in Fig. 4(d). The quantitative comparison results of the mean miss distance and the mean passing angle over all waypoints under different guidance laws for this scenario are summarized in Table IV. From this table, it can be concluded that the autopilot lag has adverse

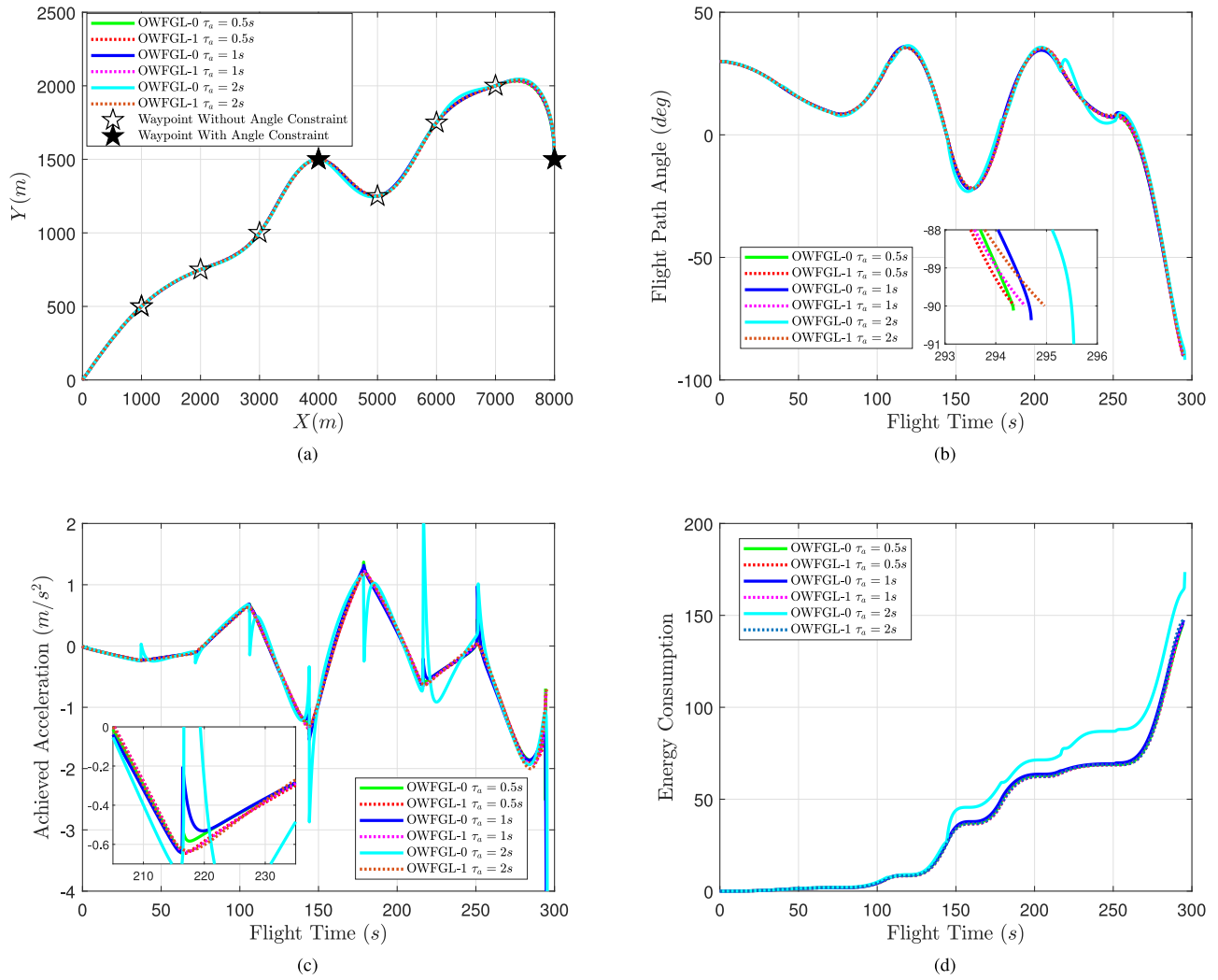


Fig. 4. Comparison results of the proposed guidance laws with different autopilot lags. (a) Flight trajectory. (b) Flight path angle. (c) Acceleration response. (d) Energy consumption.

TABLE IV
Comparison Results of the Mean Miss Distance and the Passing Angle Error

Metric	$\tau_a = 0.5s$		$\tau_a = 1s$		$\tau_a = 2s$	
	OWFGL-0	OWFGL-1	OWFGL-0	OWFGL-1	OWFGL-0	OWFGL-1
Mean miss distance	0.3887m	0.1771m	0.9901m	0.1819m	2.4409m	0.1903m
Mean passing angle error	0.2377°	0.0239°	0.5977°	0.0951°	2.001°	0.1675°

effects on the guidance accuracy, and the performance of OWFGL-0 degrades with the increase of autopilot lag.

Now, let us investigate the performance of the proposed guidance law under various UAV speeds $V = 30, 60$, and 90 m/s with a fixed autopilot lag $\tau = 0.5$ s. The comparison results, including UAV flight trajectories, flight angle profiles, achieved acceleration, and energy consumption, are depicted in Fig. 5. From this figure, we clearly observe that the performance of OWFGL-0 degrades with the increase of UAV speed. This can be attributed to the fact that the UAV has less time to initiate a response to the path change with higher flying velocity. As a comparison, the performance

of OWFGL-1 remains consistent across a wide range of UAV speeds as the autopilot lag is actively compensated in the guidance command. The quantitative comparison results of the mean miss distance and the mean passing angle over all waypoints under different guidance laws for this scenario are summarized in Table V. From this table, it can be noted that the performance of OWFGL-0 is close to OWFGL-1 for UAVs with low speed. However, the performance discrepancy between these two guidance laws drastically increases with the increase of UAV speed.

Based on the numerical simulations, it can be concluded that the proposed guidance law can effectively compensate

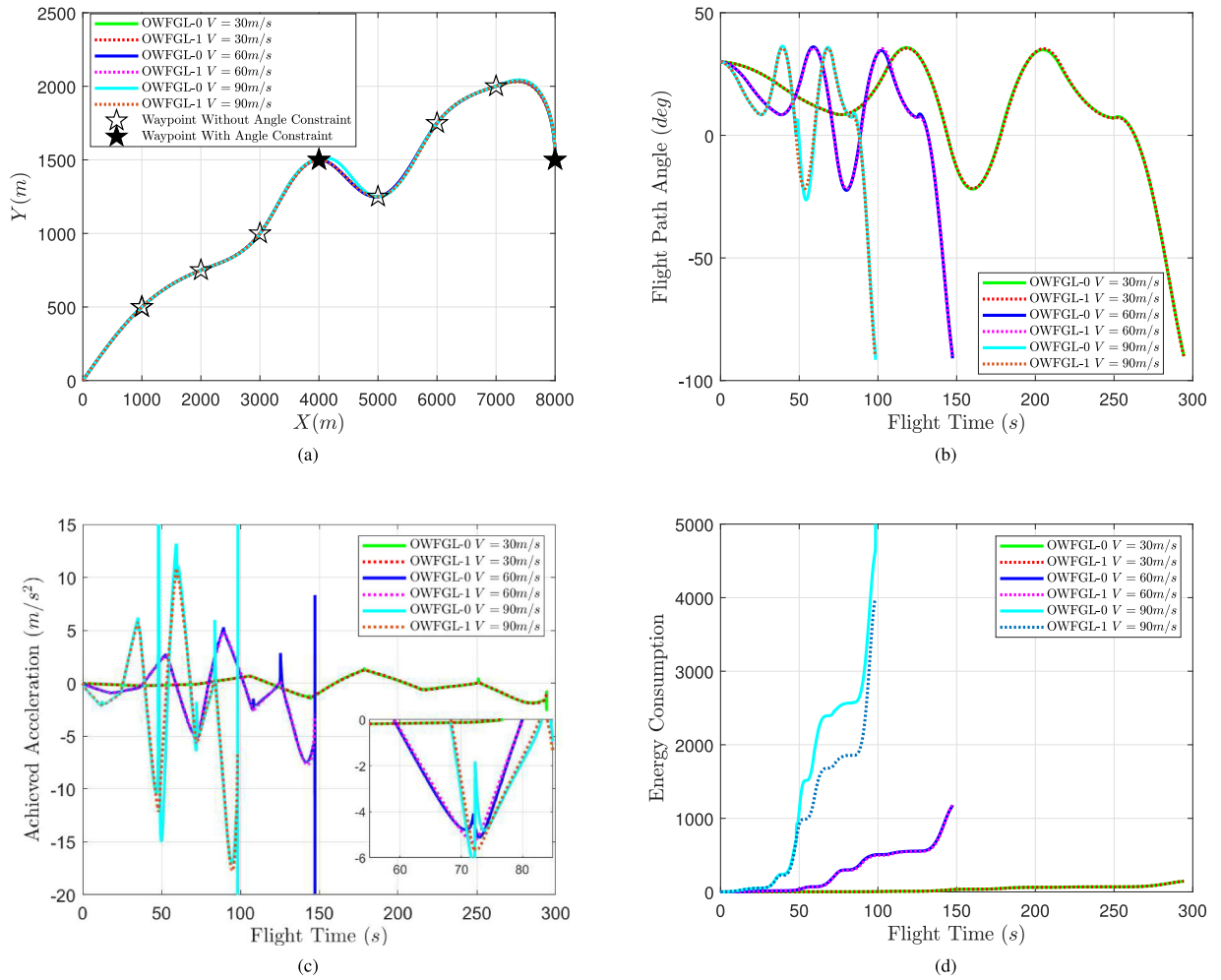


Fig. 5. Comparison results of the proposed guidance laws with flying speed. (a) Flight trajectory. (b) Flight path angle. (c) Acceleration response. (d) Energy consumption.

TABLE V
Comparison Results of the Mean Miss Distance and the Passing Angle Error

Metric	$V = 30m/s$		$V = 60m/s$		$V = 90m/s$	
	OWFGL-0	OWFGL-1	OWFGL-0	OWFGL-1	OWFGL-0	OWFGL-1
Mean miss distance	0.3887m	0.1771m	1.5165m	0.2278m	3.7727m	0.7283m
Mean passing angle error	0.2377°	0.0239°	1.3371°	0.1161°	2.3369°	0.2069°

for the autopilot lag and provide performance improvement, especially for UAVs with large time lag or high flying speed. Also, it is beneficial to compensate the autopilot delay when the range between consecutive waypoints is short due to limited response time for path change.

VII. CONCLUSION

In this article, we suggested a new energy-optimal waypoint-following guidance law for a UAV with a general autopilot system. Unlike existing numerical waypoint-following guidance, the proposed approach was derived analytically through rigorous optimal control theory. We also theoretically showed that the proposed guidance law encompassed previously suggested optimal point-to-point

guidance laws. The proposed guidance law was generic and, therefore, could be applied to general waypoint-following missions. However, the computational complexity increased with the increase of the number of boundary constraints. Nonlinear numerical comparisons clearly revealed that the proposed guidance law helped increase the endurance of the UAV and effectively compensated for the autopilot lag.

By exploiting the advantages of the proposed approach, the guidance law developed can also be applied to waypoint navigation during the midcourse guidance phase of cruise missiles and sea-skimming antiship missiles. Another potential application of the proposed guidance law is handover between midcourse and terminal course of guided weapons, i.e., $N = 2$ and $M = 0$, since the proposed guidance law

can help reduce the transient effect, as confirmed by the numerical simulations. Also, comparing the performance of energy-optimal and time-optimal waypoint guidance in consideration of acceleration bound is an interesting direction to be explored in the future.

APPENDIX A

LEMMA 1

This appendix collects a useful lemma from [53] that has been utilized in the derivation of the proposed guidance laws.

LEMMA 1 Let \mathcal{H} be a Hilbert space and $\alpha_1, \alpha_2, \dots, \alpha_n$ be a set of n linearly independent vectors in \mathcal{H} . If the condition $(x, \alpha_i) = c_i, i \in \{1, 2, \dots, n\}$, with c_i being arbitrary scalars, holds among all vectors of H , then the one that has the minimum norm is given by

$$x_{\min} = \sum_{i=1}^n b_i \alpha_i \quad (76)$$

where the coefficients b_i satisfy the condition

$$\sum_{i=1}^n (\alpha_i, \alpha_j) = b_j, \quad j \in \{1, 2, \dots, n\}. \quad (77)$$

This article applies Lemma 1 to a Hilbert space $\mathcal{H} = \mathcal{L}^2[t, t_f]$ with the inner product defined as $(f, g) = \int_t^{t_f} f(\tau)g(\tau)d\tau$.

APPENDIX B

GUIDANCE COMMANDS OF SWGL AND TSWGL

This appendix provides the guidance commands of the SWGL [18], [19] and the TSWGL [20], [21] for the completeness of this article.

Both the SWGL and the TSWGL requires to place a synthetic waypoint or a virtual target that travels along the flight path between designated inertial waypoints. Define (x_w, y_w) as the 2-D inertial position of the synthetic waypoint. The kinematics constraint of the synthetic waypoint can then be mathematically formulated as

$$\begin{aligned} \dot{x}_w &= V_w \cos \theta_f \\ \dot{y}_w &= V_w \sin \theta_f \end{aligned} \quad (78)$$

where θ_f is the reference heading between fixed waypoints, and V_w denotes the moving speed of the synthetic waypoint, governed by

$$V_w = V \frac{R}{R^*} \quad (79)$$

where R stands for the relative distance, or the so-called look-ahead distance, between the UAV and the synthetic waypoint, and R^* represents the desired look-ahead distance.

The desired relative distance R^* is defined by the UAV speed and time prediction horizon as

$$R^* = VT_p \quad (80)$$

where T_p specifies the desired time horizon that initiates a response to flight path change, which is analogous to the prediction horizon in MPC.

The SWGL applies pure pursuit missile guidance to follow the synthetic waypoint, i.e., the guidance command is given by

$$a_c = V\dot{\sigma}_w \quad (81)$$

where $\dot{\sigma}_w$ is the LoS rate between the UAV and the synthetic waypoint, which is determined as

$$\dot{\sigma}_w = \frac{1}{R}V_w \sin(\theta_f - \sigma_w) - \frac{1}{R}V \sin(\theta - \sigma_w). \quad (82)$$

Unlike the SWGL, the TSWGL employs energy-optimal trajectory shaping guidance to follow the synthetic waypoint using guidance command

$$a_c = \frac{V^2}{R} (6\sigma_w - 4\theta - 2\theta_f). \quad (83)$$

REFERENCES

- [1] R. Rysdyk
Unmanned aerial vehicle path following for target observation in wind
J. Guid., Control, Dyn., vol. 29, no. 5, pp. 1092–1100, 2006.
- [2] R. W. Beard, J. Ferrin, and J. Humpherys
Fixed wing UAV path following in wind with input constraints
IEEE Trans. Control Syst. Technol., vol. 22, no. 6, pp. 2103–2117, Nov. 2014.
- [3] Y. A. Kapitanuk, A. V. Proskurnikov, and M. Cao
A guiding vector-field algorithm for path-following control of nonholonomic mobile robots
IEEE Trans. Control Syst. Technol., vol. 26, no. 4, pp. 1372–1385, Jul. 2018.
- [4] J. L. G. Olavo, G. D. Thums, T. A. Jesus, L. C. de Araújo Pimenta, L. A. B. Torres, and R. M. Palhares
Robust guidance strategy for target circulation by controlled UAV
IEEE Trans. Aerosp. Electron. Syst., vol. 54, no. 3, pp. 1415–1431, Jun. 2018.
- [5] H. Delingette, M. Hebert, and K. Ikeuchi
Trajectory generation with curvature constraint based on energy minimization
In *Proc. IEEE/RSJ Int. Workshop Intell. Robots Syst.*, 1991, pp. 206–211.
- [6] I. Spangelo and O. Egeland
Generation of energy-optimal trajectories for an autonomous underwater vehicle
In *Proc. IEEE Int. Conf. Robot. Autom.*, 1992, pp. 2107–2112.
- [7] G. Moon and Y. Kim
Optimum flight path design passing through waypoints for autonomous flight control system
In *Proc. AIAA Guid., Navigat., Control Conf. Exhib.*, 2003, Art. no. AIAA 2003-5334.
- [8] A. Kaplan, N. Kingry, P. Uhing, and R. Dai
Time-optimal path planning with power schedules for a solar-powered ground robot
IEEE Trans. Autom. Sci. Eng., vol. 14, no. 2, pp. 1235–1244, Apr. 2017.
- [9] M. D. Zollars, R. G. Cobb, and D. J. Grymin
Optimal path planning for SUAS waypoint following in urban environments
In *Proc. IEEE Aerosp. Conf.*, 2018, pp. 1235–1244.

- [10] M. Ataei and A. Yousefi-Koma
Three-dimensional optimal path planning for waypoint guidance of an autonomous underwater vehicle
Robot. Auton. Syst., vol. 67, pp. 23–32, 2015.
- [11] G. Garcia and S. Keshmiri
Nonlinear model predictive controller for navigation, guidance and control of a fixed-wing UAV
In *Proc. AIAA Guid., Navigat., Control Conf.*, 2011, Art. no. AIAA 2011-6310.
- [12] S. He, H.-S. Shin, and A. Tsourdos
Trajectory optimization for target localization with bearing-only measurement
IEEE Trans. Robot., vol. 35, no. 3, pp. 653–668, Jun. 2019.
- [13] D. R. Nelson, D. B. Barber, T. W. McLain, and R. W. Beard
Vector field path following for miniature air vehicles
IEEE Trans. Robot., vol. 23, no. 3, pp. 519–529, Jun. 2007.
- [14] S. Park, J. Deyst, and J. P. How
A new nonlinear guidance logic for trajectory tracking
In *Proc. AIAA Guid., Navigation, Control Conf. Exhib.*, 2004, Art. no. AIAA 2004-4900.
- [15] S. Park, J. Deyst, and J. P. How
Performance and Lyapunov stability of a nonlinear path following guidance method
J. Guid., Control, Dyn., vol. 30, no. 6, pp. 1718–1728, 2007.
- [16] N. Cho, Y. Kim, and S. Park
Three-dimensional nonlinear differential geometric path-following guidance law
J. Guid., Control, Dyn., vol. 38, no. 12, pp. 2366–2385, 2015.
- [17] M. Kothari, I. Postlethwaite, and D.-W. Gu
UAV path following in windy urban environments
J. Intell. Robot. Syst., vol. 74, nos. 3/4, pp. 1013–1028, 2014.
- [18] E. D. Medagoda
Closed loop stability of synthetic waypoint guidance algorithm
IFAC Proc. Vol., vol. 43, no. 15, pp. 75–80, 2010.
- [19] E. D. B. Medagoda and P. W. Gibbens
Synthetic-waypoint guidance algorithm for following a desired flight trajectory
J. Guid., Control, Dyn., vol. 33, no. 2, pp. 601–606, 2010.
- [20] A. Ratnoo, S. Hayoun, A. Granot, and T. Y. Shima
Path following using trajectory shaping guidance
In *Proc. AIAA Guid., Navigat., Control Conf.*, 2013, Art. no. AIAA 2013-5233.
- [21] A. Ratnoo, S. Y. Hayoun, A. Granot, and T. Shima
Path following using trajectory shaping guidance
J. Guid., Control, Dyn., vol. 38, no. 1, pp. 106–116, 2014.
- [22] R. G. Cottrell
Optimal intercept guidance for short-range tactical missiles
AIAA J., vol. 9, no. 7, pp. 1414–1415, 1971.
- [23] P. Zarchan
Tactical and Strategic Missile Guidance. Washington, DC, USA: Amer. Inst. Aeronaut. Astronaut., 2012.
- [24] C.-K. Ryoo, H. Cho, and M.-J. Tahk
Optimal guidance laws with terminal impact angle constraint
J. Guid., Control, Dyn., vol. 28, no. 4, pp. 724–732, 2005.
- [25] C.-K. Ryoo, H. Cho, and M.-J. Tahk
Time-to-go weighted optimal guidance with impact angle constraints
IEEE Trans. Control Syst. Technol., vol. 14, no. 3, pp. 483–492, May 2006.
- [26] S. He and C.-H. Lee
Optimal impact angle guidance for exoatmospheric interception utilizing gravitational effect
IEEE Trans. Aerosp. Electron. Syst., vol. 55, no. 3, pp. 1382–1392, Jun. 2019.
- [27] E. W. Frew, J. Langelaan, and S. Joo
Adaptive receding horizon control for vision-based navigation of small unmanned aircraft
In *Proc. Amer. Control Conf.*, 2006, p. 6.
- [28] T. Keviczky and G. J. Balas
Flight test of a receding horizon controller for autonomous UAV guidance
In *Proc. IEEE Amer. Control Conf.*, 2005, pp. 3518–3523.
- [29] J. Sprinkle, J. M. Eklund, H. J. Kim, and S. Sastry
Encoding aerial pursuit/evasion games with fixed wing aircraft into a nonlinear model predictive tracking controller
In *Proc. 43rd IEEE Conf. Decis. Control*, 2004, vol. 3, pp. 2609–2614.
- [30] I. H. Whang and T. W. Hwang
Horizontal waypoint guidance design using optimal control
IEEE Trans. Aerosp. Electron. Syst., vol. 38, no. 3, pp. 1116–1120, Jul. 2002.
- [31] C.-K. Ryoo, H.-S. Shin, and M.-J. Tahk
Energy optimal waypoint guidance synthesis for antiship missiles
IEEE Trans. Aerosp. Electron. Syst., vol. 46, no. 1, pp. 80–95, Jan. 2010.
- [32] L. E. Dubins
On curves of minimal length with a constraint on average curvature, and with prescribed initial and terminal positions and tangents
Amer. J. Math., vol. 79, no. 3, pp. 497–516, 1957.
- [33] T. G. McGee and J. K. Hedrick
Optimal path planning with a kinematic airplane model
J. Guid., Control, Dyn., vol. 30, no. 2, pp. 629–633, 2007.
- [34] L. Techy and C. A. Woolsey
Minimum-time path planning for unmanned aerial vehicles in steady uniform winds
J. Guid., Control, Dyn., vol. 32, no. 6, pp. 1736–1746, 2009.
- [35] S. Hota and D. Ghose
Optimal trajectory planning for unmanned aerial vehicles in three-dimensional space
J. Aircr., vol. 51, no. 2, pp. 681–688, 2014.
- [36] P. Bauer and A. Dorobantu
Optimal waypoint guidance, trajectory design and tracking
In *Proc. Amer. Control Conf.*, 2013, pp. 812–817.
- [37] H. Hindi, L. Crawford, R. Zhou, and C. Eldershaw
Efficient waypoint tracking hybrid controllers for double integrators using classical time optimal control
In *Proc. 47th IEEE Conf. Decis. Control*, 2008, pp. 5662–5667.
- [38] S. Manyam, S. Rathinam, and D. Casbeer
Dubins paths through a sequence of points: Lower and upper bounds
In *Proc. IEEE Int. Conf. Unmanned Aircr. Syst.*, 2016, pp. 284–291.
- [39] S. G. Manyam, S. Rathinam, D. Casbeer, and E. Garcia
Tightly bounding the shortest Dubins paths through a sequence of points
J. Intell. Robot. Syst., vol. 88, no. 2–4, pp. 495–511, 2017.
- [40] S. Hota and D. Ghose
Optimal trajectory generation for convergence to a rectilinear path
J. Intell. Robot. Syst., vol. 75, no. 2, pp. 223–242, 2014.
- [41] S. Hota and D. Ghose
Optimal trajectory planning for path convergence in three-dimensional space
Proc. Inst. Mech. Eng., Part G: J. Aerosp. Eng., vol. 228, no. 5, pp. 766–780, 2014.
- [42] S. He and C.-H. Lee
Optimal proportional-integral guidance with reduced sensitivity to target maneuvers
IEEE Trans. Aerosp. Electron. Syst., vol. 54, no. 5, pp. 2568–2579, Oct. 2018.
- [43] S. He and C.-H. Lee
Optimality of error dynamics in missile guidance problems
J. Guid., Control, Dyn., vol. 41, no. 7, pp. 1624–1633, 2018.

- [44] B. Jha, R. Tsalik, M. Weiss, and T. Shima
Cooperative guidance and collision avoidance for multiple pursuers
J. Guid., Control, Dyn., vol. 42, no. 7, pp. 1506–1518, 2019.
- [45] M. Weiss and T. Shima
Linear quadratic optimal control-based missile guidance law with obstacle avoidance
IEEE Trans. Aerosp. Electron. Syst., vol. 55, no. 1, pp. 205–214, Feb. 2019.
- [46] M. Weiss, T. Shima, D. Castaneda, and I. Rusnak
Combined and cooperative minimum-effort guidance algorithms in an active aircraft defense scenario
J. Guid., Control, Dyn., vol. 40, no. 5, pp. 1241–1254, 2017.
- [47] A. E. Bryson
Applied Optimal Control: Optimization, Estimation and Control. Evanston, IL, USA: Routledge, 2018.
- [48] V. Shaferman and T. Shima
Linear quadratic guidance laws for imposing a terminal intercept angle
J. Guid., Control, Dyn., vol. 31, no. 5, pp. 1400–1412, 2008.
- [49] S. Y. Hayoun, M. Weiss, and T. Shima
A mixed l_2/l_α differential game approach to pursuit-evasion guidance
IEEE Trans. Aerosp. Electron. Syst., vol. 52, no. 6, pp. 2775–2788, Dec. 2016.
- [50] T. Shima and O. M. Golan
Linear quadratic differential games guidance law for dual controlled missiles
IEEE Trans. Aerosp. Electron. Syst., vol. 43, no. 3, pp. 834–842, Jul. 2007.
- [51] I. Taub and T. Shima
Intercept angle missile guidance under time varying acceleration bounds
J. Guid., Control, Dyn., vol. 36, no. 3, pp. 686–699, 2013.
- [52] C.-H. Lee, H.-S. Shin, J.-I. Lee, and M.-J. Tahk
Zero-effort-miss shaping guidance laws
IEEE Trans. Aerosp. Electron. Syst., vol. 54, no. 2, pp. 693–705, Apr. 2018.
- [53] D. G. Luenberger
Optimization by Vector Space Methods. Hoboken, NJ, USA: Wiley, 1997.



Shaoming He received the B.Sc. and M.Sc. degrees in aerospace engineering from the Beijing Institute of Technology, Beijing, China, in 2013 and 2016, respectively. He is currently working toward the Ph.D. degree in aerospace engineering with the School of Aerospace, Transport and Manufacturing, Cranfield University, Cranfield, U.K.

His research interests include multitarget tracking, unmanned aerial vehicle guidance, and trajectory optimization.



Hyo-Sang Shin received the B.Sc. degree in aerospace engineering from Pusan National University, Busan, South Korea, in 2004, the M.Sc. degree in flight dynamics, guidance, and control in aerospace engineering from the Korea Advanced Institute of Science and Technology, Daejeon, South Korea, in 2006, and the Ph.D. degree in cooperative missile guidance from Cranfield University, Cranfield, U.K., in 2010.

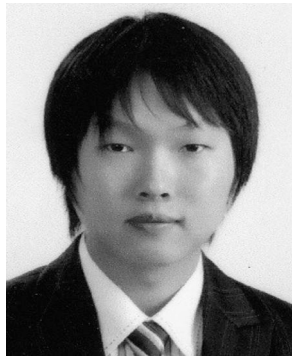
He is currently Reader on Guidance, Control, and Navigation Systems with the Autonomous and Intelligent Systems Group, Cranfield University. His current research interests include multiple target tracking, probabilistic target detection, and distributed control of multiple agent systems.



Antonios Tsourdos received the M.Eng. degree in electronic, control, and systems engineering from the University of Sheffield, Sheffield, U.K., in 1995, the M.Sc. degree in systems engineering from Cardiff University, Cardiff, U.K., in 1996, and the Ph.D. degree in nonlinear robust missile autopilot design and analysis from Cranfield University, Cranfield, U.K., in 1999.

He is currently a Professor of Control Engineering with Cranfield University, where he became the Head of the Centre for Cyber-Physical Systems in 2013.

Dr. Tsourdos was a member of the Team Stellar, the winning team for the U.K. Ministry of Defence Grand Challenge (2008) and the IET Innovation Award (Category Team, 2009).



Chang-Hun Lee received the B.S., M.S., and Ph.D. degrees in aerospace engineering from the Korea Advanced Institute of Science and Technology (KAIST), Daejeon, South Korea, in 2008, 2010, and 2013, respectively.

From 2013 to 2015, he was a Senior Researcher with the Guidance and Control Team, Agency for Defense Development, Daejeon. From 2016 to 2018, he was a Research Fellow with the School of Aerospace, Transportation, and Manufacturing, Cranfield University, Cranfield, U.K. Since 2019, he has been with the Department of Aerospace Engineering, KAIST, where he is currently an Assistant Professor. His recent research interests include advanced missile guidance and control, cooperative control for unmanned aerial vehicles, target tracking filters, deep learning, and aviation data analytics.

Dr. Lee is an Associate Editor for the *International Journal of Aeronautical and Space Science*.

2019-11-28

Energy-optimal waypoint-following guidance considering autopilot dynamics

He, Shaoming

IEEE

He S, Shin H-S, Tsourdos A, Lee C-H. (2020) Energy-optimal waypoint-following guidance considering autopilot dynamics. IEEE Transactions on Aerospace and Electronic Systems, Volume 56, Issue 4, August 2020, pp. 2701-2717

<https://doi.org/10.1109/TAES.2019.2954149>

Downloaded from Cranfield Library Services E-Repository